frontiers | Frontiers in Earth Science

TYPE Original Research
PUBLISHED 14 May 2024
DOI 10.3389/feart.2024.1354238

OPEN ACCESS

EDITED BY
Bin Gong,
Brunel University London, United Kingdom

REVIEWED BY
Mohammad Azarafza,
University of Tabriz, Iran
Xun Xi,
University of Science and Technology Beijing, China

*CORRESPONDENCE
Junjun Jiang,
jiangjunjun21@163.com

RECEIVED 12 December 2023
ACCEPTED 09 April 2024
PUBLISHED 14 May 2024

CITATION
Jiang J, Deng Z, Zhang G and Yang S (2024), A case study for coupling mechanism of anti-rockburst and pressure relief in gas drainage borehole along seam.
Front. Earth Sci. 12:1354238.
doi: 10.3389/feart.2024.1354238

A case study for coupling mechanism of anti-rockburst and pressure relief in gas drainage borehole along seam

Junjun Jiang[1,2,3]*, Zhigang Deng[2,3], Guanghui Zhang[2,3] and Shengli Yang[1]

[1]School of Energy and Mining Engineering, China University of Mining and Technology (Beijing), Beijing, China, [2]China Coal Research Institute, Beijing, China, [3]State Key Laboratory of Coal Mine Disaster Prevention and Control, Beijing, China

After high gas mines coal mining reaches deep, the issue of rockburst has become increasingly prominent. Aiming at solving the problem of rock burst in high gas mines, the coupling mechanism of anti-rockburst and pressure relief in gas drainage boreholes along seam has been explored. The research results indicate that gas drainage boreholes can reduce the stress environment of coal, making the peak stress transfer to deep coal. The pressure relief effect of gas drainage boreholes is slightly weaker than that of large diameter pressure relief boreholes. Moreover, the presence of gas pressure can weaken the mechanical properties of coal. The compressive strength, elastic modulus, cohesion, and internal friction angle of coal all show varying degrees of attenuation with the increase of gas pressure. Besides, a stress analysis was conducted on borehole surrounding rock, and mathematical derivation was also carried out. The expressions for radial stress and circumferential stress of the coal at the boundary of the plastic zone of the borehole surrounding rock, as well as the analytical solution for the boundary of the plastic zone, are obtained. In addition, the gas in pressure relief borehole act on the coal in the pressure relief zone, causing deterioration of the mechanical properties of the coal around the pressure relief boreholes. The expansion range of the radius of the borehole pressure relief zone will increases, and the borehole pressure relief effect will enhance, promoting the formation of coal weakening zones. The above is the coupling mechanism of anti-rockburst and pressure relief in gas drainage boreholes, which has been confirmed by numerical simulation for reliability.

KEYWORDS

gas coal seam, compound disaster, gas drainage borehole, gas pressure, anti-rockburst and pressure relief, coupling mechanism

Highlights

- From the perspective of pressure relief, drainage boreholes can reduce the stress environment of coal and further transfer the peak stress of coal to deep coal.
- The compressive strength, elastic modulus, cohesion, and internal friction angle of coal all show varying degrees of attenuation with the increase of gas pressure.
- By conducting stress analysis on the surrounding rock of the boreholes and mathematical derivation, the radial and circumferential stress expressions of the

boundary coal in the plastic zone of the boreholes surrounding rock were obtained.
- The coupling mechanism of anti-rockburst and pressure relief in gas drainage boreholes had been investigated, which has been confirmed by numerical simulation for reliability.

1 Introduction

After coal mining reaches deep, the coal seams exhibit increasingly pronounced features such as high ground stress, strong gas adsorption, and low permeability, resulting in significant changes to the mining environment (Xie et al., 2012). Consequently, as the depth of coal resource extraction increases, some mines encounter the dual hazards of rockburst and gas outburst, which are characterized by their mutual induction and compounding effects (Yuan 2015). When subjected to external stresses, coal and rock undergo not only the instantaneous release of elastic deformation energy but also the abrupt discharge of gas. This phenomenon manifests as a compound dynamic disaster, exhibiting both the characteristics of a rockburst and gas emission simultaneously (Wang et al., 2014; Pan 2016; Qi et al., 2020a; Li et al., 2021). Notably, mines such as Pingdingshan Coal Industry Group No. 10 Mine, Fushun Laohutai Coal Mine, Hegang Coal Field, Fuxin Mining Company Wulong Coal Mine, Wangying Coal Mine, and Sunjiawan Coal Mine in China have experienced rockbursts accompanied by abnormal gas emissions, occasionally leading to the induction of gas-related disasters.

The safety issue of gas drainage is prominent. Moreover, after entering deep, it is also necessary to consider the problem of rockburst. Disaster prevention and control have become increasingly challenging, seriously affecting the safety of coal mine production. The current rockburst mitigation framework, while relatively advanced, relies heavily on the integration of regional preventative measures with localized risk-mitigation strategies. Both centered around the fundamental objective of stress redistribution and avoidance of stress concentrations. This holistic approach is essential in effectively tackling the challenges posed by rockburst events. (Yuan et al., 2015; Wang and Chen, 2018; Ali et al., 2023). Localized risk-mitigation efforts specifically target the roof, coal seam, and floor, employing a range of pressure-relief techniques such as large-diameter drilling, coal seam blasting, roof deep-hole blasting, hydraulic fracturing, and directional fracturing, among others. These methods aim to disrupt the structural integrity of hard coal seams and surrounding rock strata, facilitating the release of accumulated stress within impact hazard zones and thereby reducing the likelihood of rockburst occurrences. At present, regional outburst prevention strategies encompass two primary techniques: protective layer mining and extensive pre-drainage of coal seam gas. These methods, when combined with refined local outburst prevention measures including pre-drainage of gas, advance drilling, hydraulic interventions, and controlled blasting, constitute a comprehensive and robust outburst prevention system (Cheng et al., 2004). In scenarios involving single coal seams, outburst-prone protective layers, or unprotected regions within protected layers, the pre-drainage of coal seam gas emerges as a particularly effective technique for enhancing mining safety.

Currently, pre-drainage methods are commonly used to control coal seam gas in high gas mines, outburst mines, and high gas areas of low gas mines in China. Numerous practices have shown that gas pre-drainage of coal seam is an effective measure for gas control, and it has become the main means to prevent gas outburst and reduce gas emission quantity (Wang et al., 2014). Compared to other pre-drainage methods for coal seam gas control, the drainage borehole along seam has the advantages of simple arrangement process, fast drilling speed, and low cost. Therefore, gas pre–drainage borehole along seam has become the mainstream measure for coal seam gas control. When construction conditions permit, pre–drainage borehole along seam has been widely used as the preferred construction method for gas pre-drainage boreholes in Chinese coal mines (Pan, 2016). Some scholars have conducted research on the correlation between increasing the diameter of drainage boreholes and drainage volume through experiments and numerical simulations. It has been found that the relationship between the drainage volume and the diameter of the drainage borehole shows an initial increase (approximately linear) followed by a stable trend (Cai and Zhou, 2002; Ding et al., 2008; Xu et al., 2010; Liu et al., 2021). Large diameter boreholes significantly disrupt the surrounding coal seams, leading to a widespread distribution of fractures and the development of numerous cracks in their vicinity. There are multiple and interconnected channels for gas desorption and release, which greatly reduces the gas pressure inside the coal seam and increases the plasticity of the coal. Therefore, it is more conducive to gas drainage. Drilling long boreholes with large diameter in stable coal seams can not only save costs, but also improve the efficiency of drilling and gas drainage, which is of great significance for mine safety production. Meanwhile, conducting large diameter boreholes in coal can also partially release the elastic energy accumulated in the coal. The concentrated stress zone in the mining space will be forced to transfer to the deep, reducing the degree of concentrated stress (Huang et al., 2016; Zhang et al., 2019; Zhao et al., 2020; Wang et al., 2021).

The core of rock burst prevention and control is stress transfer and stress release. This is achieved by modifying the stress conditions within coal and rock masses or mitigating the development of excessive stress concentrations, thereby ensuring their stability and preventing any potential destabilizing or catastrophic failures (Qi et al., 2019; Qi et al., 2020b). However, the fundamental measure for controlling gas coal seams is gas drainage, and pressure relief and permeability enhancement play a crucial role (Yu and Wang, 2005; Shi et al., 2009; Wang et al., 2022). In a sense, the points of departure for their prevention and control are different. Nevertheless, there are some similarities in the prevention and control methods for the mining working face. For example, the gas drainage along seam and the pressure relief through large diameter boreholes in the mining working face are both drilling borehole in coal seams. It is just that the process parameters are different (Liu et al., 2007; Lei and Sun, 2010; Huang and Jiang, 2011; Wang et al., 2011; Jia et al., 2017; Shi et al., 2017).

At present, there is still far from enough theoretical research on the use of gas drainage boreholes along seam for anti-rockburst and pressure relief in coal seam. The requirements for guiding the prevention and control of rockburst disasters in gas coal seam cannot be met. Therefore, this article starts from reality and takes deep high gas coal seams as the research

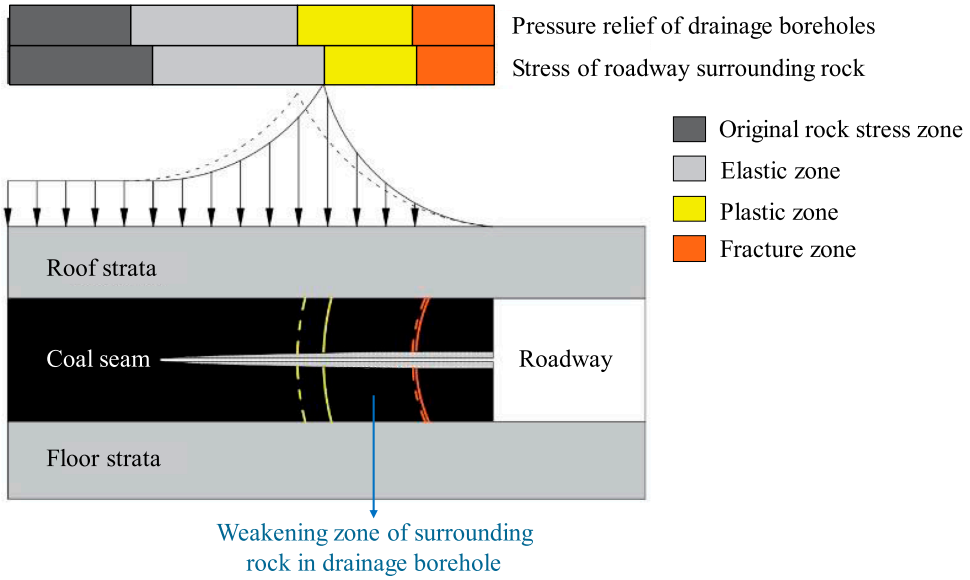

FIGURE 1
Schematic diagram of stress characteristics for roadway surrounding rock.

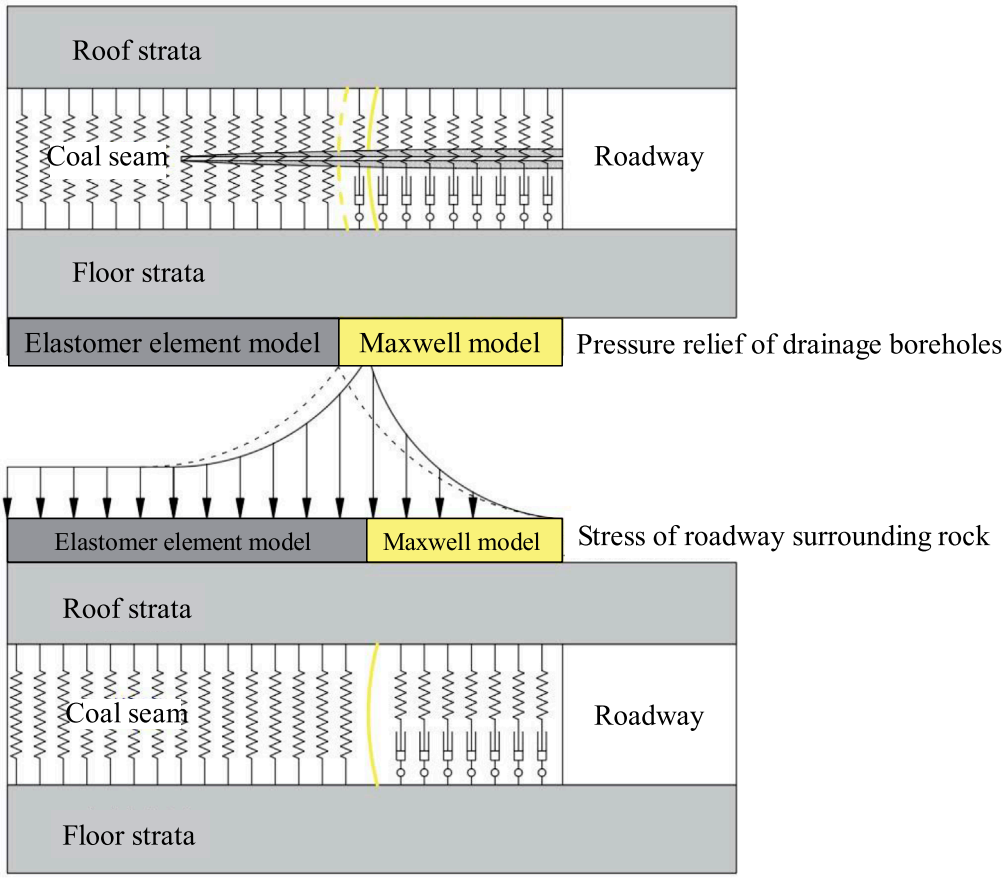

FIGURE 2
Schematic diagram of mechanical model of roadway surrounding rock.

TABLE 1 Physical and mechanical parameters of each rock layer in the model.

Rock layer	Rock properties	Thickness (m)	Density ($kg \cdot m^{-3}$)	Shear modulus (GPa)	Bulk modulus (GPa)	Cohesive force (MPa)	The angle of internal friction (°)
1	Roof strata	20	2,503	18.9	9.73	8.2	31.4
2	Coal seam	4.9	1,400	1.47	0.86	3.1	27.1
3	Floor strata	12	2,475	6.62	5.82	7.6	29.0

object. Through laboratory experiments, theoretical calculations, numerical simulations, and other means, the coupling mechanism of gas drainage boreholes for anti-rockburst and pressure relief is studied. It will have significant practical significance to guide the prevention and control of rockburst disasters in gas coal seam.

2 Feasibility analysis of pressure relief in drainage boreholes along seam

2.1 Feasibility analysis of pressure relief in drainage boreholes along seam

Before roadway tunnelling, the coal seam is in a state of original rock stress, and the gravity of the overburden rock is uniformly distributed on the coal seam. After roadway tunnelling, the stress in the surrounding rock is redistributed, which can be divided into broken zone, plastic zone, elastic zone, and original rock stress zone according to the different states of the coal, as shown in Figure 1. The coal situated between the roadway surface and the elastic-plastic stress boundary exists in a state of limit equilibrium. In mines with high gas outbursts, gas drainage is facilitated by drilling holes along the seam during both roadway tunnelling and extraction at the working face. On the one hand, gas drainage boreholes along seam in the roadway can extract the remaining gas in the coal seam. In addition, due to the concentration of stress around the borehole, a small-scale weakening zone of the borehole surrounding rock will form around the borehole (Figure 1). As a result, the mechanical structure of the roadway surrounding rock will be changed (Ma et al., 2020; Pang et al., 2021).

According to the whole stress-strain curve of coal, the coal exhibits strain softening characteristics during the post peak failure stage (Zhang, 1987), which is similar to the mechanical properties of coal in the failure zone and plastic zone of the roadway surrounding rock. Therefore, the simulation can be carried out by connecting viscous and elastic components in series (Maxwell model). The elastic zone and original rock stress zone of the roadway surrounding rock are simulated using completely elastic components, as illustrated in Figure 2, which presents a mechanical model of the tunnel's surrounding rock. The load capacity of the coal seam is damaged by the weakening zone of the surrounding rock in gas drainage borehole, which changes the mechanical structure of the roadway surrounding rock. Thus, some areas of the elastic zone in the roadway surrounding rock transition from the elastic zone to the plastic zone, and the range of the plastic zone increases. Moreover, the elastic component model is transformed into the Maxwell model. In the process of roof subsidence and floor heave deformation, the deformation of coal is absorbed by the viscous component in Maxwell model. This reduces the stress on the coal and gradually reaches its limit with the deformation of the viscous components. The elastic components in the Maxwell model undergo deformation, gradually increasing the stress on the coal. In summary, it can be seen that under the action of the weakening zone of the surrounding rock in the gas drainage borehole, the peak stress of the roadway surrounding rock shifts towards the depth.

2.2 The influence of drainage boreholes along seam on the stress of roadway surrounding rock

Taking a high gas mine in Shanxi Province as the background, numerical simulation was conducted on the pressure relief effect of coal in for gas drainage boreholes along seam using COMSOL numerical simulation software. The physical dimensions of the model are 105.0, 6.0, and 36.9 m in length, width, and height, respectively. The thickness of the coal seam, roof strata, and floor strata is 4.9, 20.0, and 12.0 m, respectively. The vertical stress of 15 MPa is applied to the upper boundary of the model, and roller supports are used for other boundaries. Three different drilling projects were designed. There is no borehole in scheme I. The large diameter pressure relief boreholes along seam were installed in scheme II, with a drilling length of 15 m, a drilling diameter of 150 mm and a drilling spacing of 1.5 m. The deep extraction boreholes were carried out at the inner end of the pressure relief boreholes in scheme III, with a length of 20 m and a diameter of 90 mm, forming a drainage and pressure relief boreholes along seam. Without considering the influence of gas and construction technology, numerical simulation was conducted on the pressure relief treatment effect of drainage boreholes and pressure relief boreholes by COMSOL software. The pressure relief effect of drainage boreholes was evaluated from the perspective of coal stress. The model parameters are detailed in Table 1, and the schematic diagram of the model is shown in Figure 3. The stress distribution curve of

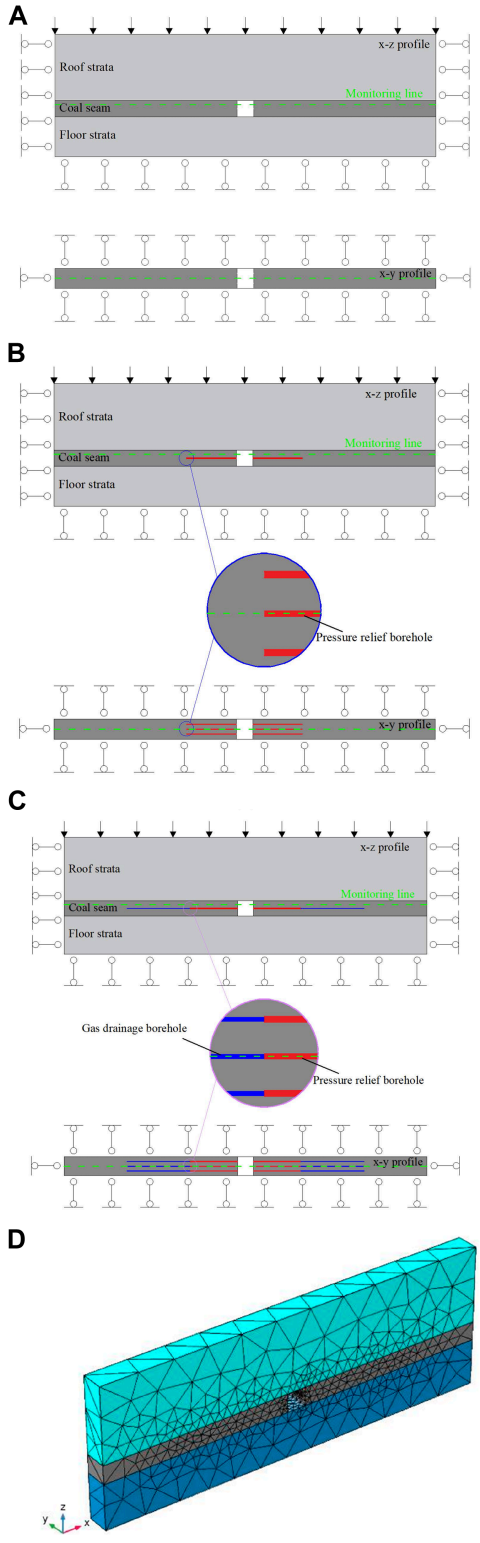

FIGURE 3
Schematic diagram of numerical model: **(A)** scheme I; **(B)** scheme II; **(C)** scheme III; **(D)** three-dimensional stereogram.

the roadway surrounding rock is drawn by extracting the stress value of the coal seam above the central borehole, as shown in Figure 4.

It can be observed from Figure 4 that the large diameter pressure relief boreholes in scheme II can effectively reduce coal seam stress within the range of drilling length (The Von Mises stress decreases by 3.1 MPa). The stress distribution of the roadway surrounding rock presents a "cup" shape with the centerline of the roadway as the axis of symmetry. At the junction between the end of the pressure relief boreholes and the coal seam, the stress in the coal seam rapidly increases and a peak stress occurs. Compared to coal seams without boreholes, the peak stress shifts towards the deeper part of the coal seam. The pressure relief effect of the large diameter pressure relief borehole in scheme III is similar to that in scheme II. However, at the junction of pressure relief borehole and drainage borehole, the stress in the coal seam slightly increases, resulting in local stress concentration. The maximum stress in the coal seam within this range is still smaller than the stress in the coal seam without boreholes. Within the range of drilling length, drainage boreholes can also effectively reduce coal seam stress. Nevertheless, due to the different pore sizes of the borehole, the effect of pressure relief is slightly worse than that of pressure relief boreholes (The Von Mises stress decreases by 2.7 MPa). At the junction between the end of the drainage boreholes and the coal seam, the coal seam stress rapidly increases and a peak stress occurs. Compared to scheme II, the peak stress further shifts towards the deep part of the coal seam. Overall, the peak stress of scheme I, II, and III gradually increases. Moreover, the peak stress of scheme II increased by 0.98 MPa compared to scheme II, while scheme III increased by 0.57 MPa compared to scheme II.

From the above, it can be seen that in scheme II, single pressure relief borehole has a strong pressure relief effect on the coal seam stress within the drilling length range, and transfers the peak stress of the coal seam to the deep part of the coal seam. In scheme III, based on the impact of pressure relief in pressure relief boreholes, the coal seam is depressurized by drainage boreholes within the length range of this borehole. The pressure relief effect of the combination of drainage and pressure relief boreholes is slightly weaker than that of large diameter pressure relief boreholes. However, compared to scheme II, the peak stress of the coal seam further shifts towards the depth of the coal seam. Therefore, drainage boreholes can also play a role in anti-rockburst and pressure relief during the process of gas extraction. The comparison results of three schemes can be seen in Table 2.

3 The influence of gas pressure on the mechanical properties of coal

3.1 Uniaxial compression test of gas coal under gas-solid coupling

Uniaxial compression tests of coal samples under different gas pressure conditions (0, 0.5, 1, 2 MPa) were conducted. Standard core plugs with a diameter of 50 mm and length of 100 mm were prepared for experiments, as shown in Figure 5. To simulate the state of the original rock gas environment, equal confining pressure and gas pressure are applied to the coal sample until the stress-strain curve no longer changes under the set gas pressure. Considering the safety of the experiment, carbon dioxide was used instead of gas. Then, the gas pressure and confining pressure

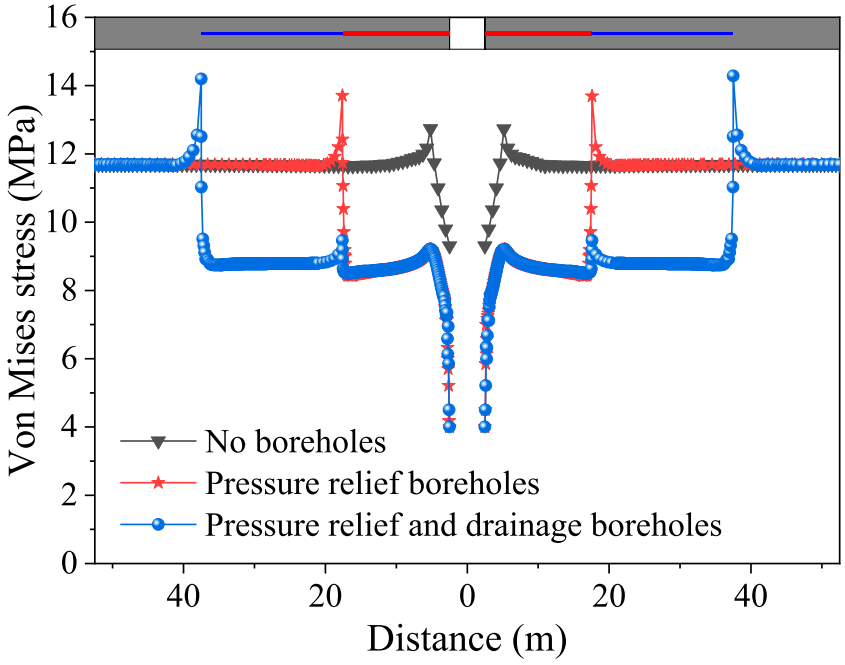

FIGURE 4
Stress distribution curves of roadway surrounding rock after construction with different drilling programs.

were sequentially removed, and the uniaxial compression test of the coal sample was carried out. Axial loading was conducted at a speed of 0.001%/s until the sample yielded. Figure 6 shows the experimental equipment. Mechanical parameters such as elastic modulus and Poisson's ratio were calculated based on the stress-strain curve of the coal sample. The peak stress during specimen failure was recorded, and the test results are listed in Table 3.

It can be seen that when the gas pressure increases from 0 to 2 MPa, the uniaxial compressive strength and elastic modulus of the samples decrease from 10.735 to 7.836 MPa and from 2.370 to 1.864 GPa, respectively, reducing by 26.9% and 21.4%. The Poisson's ratio does not show a significant change pattern. The curves of the three parameters changing with gas pressure are plotted in Figure 7. As the gas pressure increases, the strength and elastic modulus of the coal gradually decrease, and the rate of change shows a slow increasing trend.

The influence of gas on the strength of coal is the result of the combined action of free gas and adsorbed gas. Free gas acts on the coal in the form of volumetric force, reducing the effective stress of the coal and weakening its strength. Adsorbed gas has a nonmechanical effect on coal, decreasing the surface free energy of the coal. Moreover, the higher the gas pressure, the more the gas adsorption capacity of coal, and the more the free energy on the coal surface decreases, which weakens the strength of coal. As the gas pressure increases, the effective stress and compaction degree of coal weaken. The contact area on its surface reduces, resulting in a decrease in coal stiffness and elastic modulus.

3.2 Triaxial compression test of gas coal under gas-solid coupling

Triaxial compression tests of coal samples under different gas pressure conditions (0, 1, 2, 3 MPa) were carried out. Considering the safety of the test, carbon dioxide was used instead of gas. The same method as above was applied to simulate the state of the original rock gas environment. The confining pressure (σ_3) is set to 3.5, 4.4, and 5.3 MPa respectively, and loaded to the specified value at a speed of 0.5 MPa/min. Then axial loading was carried out at a speed of 0.001%/s until the samples yielded.

Figure 8 shows the failure images of coal samples under the same confining pressure and different gas pressure conditions. It is observable that the failure of coal predominantly manifests as shear failure occurring along the structural plane. The failure surface of coal becomes increasingly singular and flatter as the gas pressure increases. Additionally, there is a significant decrease in the proportion of broken coal after instability, with the broken coal exhibiting enhanced completeness. The results of coal failure indicate that gas pressure promotes the development of the failure form of coal samples from brittle failure to ductile failure. Meanwhile, the higher the gas pressure, the more obvious the ductile fracture characteristics of the coal sample.

3.3 Impact of gas pressure on coal mechanical properties

The variation of mechanical properties parameters such as triaxial strength, triaxial elastic modulus, cohesion, and

TABLE 2 The comparison results of three schemes.

No.	Borehole layout	Length of borehole (m)	Pressure relief range (m)	The effect of pressure relief
Scheme I	No borehole	0	1.5–2	Good
Scheme II	Pressure relief borehole	15	15	Fair
Scheme III	Pressure relief and drainage borehole	15+20	34.5	poor

FIGURE 5
Experimental standard coal samples.

internal friction angle of coal with gas pressure is shown in Figure 9. Under constant gas pressure, an increase in confining pressure leads to a gradual enhancement of both the triaxial compressive strength and elastic modulus of the coal. Conversely, when the confining pressure remains unchanged, the triaxial compressive strength and elastic modulus of the samples exhibit a decrease with the escalation of gas pressure. Moreover, the cohesion and internal friction angle of the samples also show a decreasing trend with the increase of gas pressure. Within a certain range, the influence of unit confining pressure on coal strength is greater than that of unit gas pressure. And the influence of unit confining pressure on elastic modulus is weaker than that of unit gas pressure. The contour curves all exhibit an upward convex shape.

Since coal belongs to heterogeneous porous medium, as the confining pressure increases, a large number of pores and fractures inside the coal are compacted and closed. Thus, the load capacity and stiffness of coal are improved, and the corresponding compressive strength and elastic modulus of coal samples gradually increase. The influence of gas pressure on the sample is in contrast to that of confining pressure. The reduction in gas pressure diminishes the effective confining pressure exerted on the coal sample, resulting in a continuous decline in both its compressive and residual strengths. Consequently, this causes a decrease in the slope of the model strength curve, which translates to a reduction in the elastic modulus.

The gas inside the coal and rock usually has free state and adsorbed state, with a dynamic interconversion occurring between the two. The mechanical strength of coal is primarily influenced by the presence of free gas, whereas other mechanical parameters, such as cohesion, are predominantly affected by adsorbed gas. As gas pressure escalates, the free gas within the coal gradually transitions into an adsorbed state, resulting in an augmentation of adsorbed gas content. Consequently, this increase in adsorbed gas leads to a diminution in the intermolecular bonding force between coal particles, ultimately manifesting as a reduction in cohesion at the macro level.

4 Coupling mechanism of anti-rockburst and pressure relief in drainage boreholes

4.1 Stress distribution of borehole surrounding rock

The stress model of the borehole surrounding rock is shown in Figure 10, where P represents the vertical pressure on the borehole

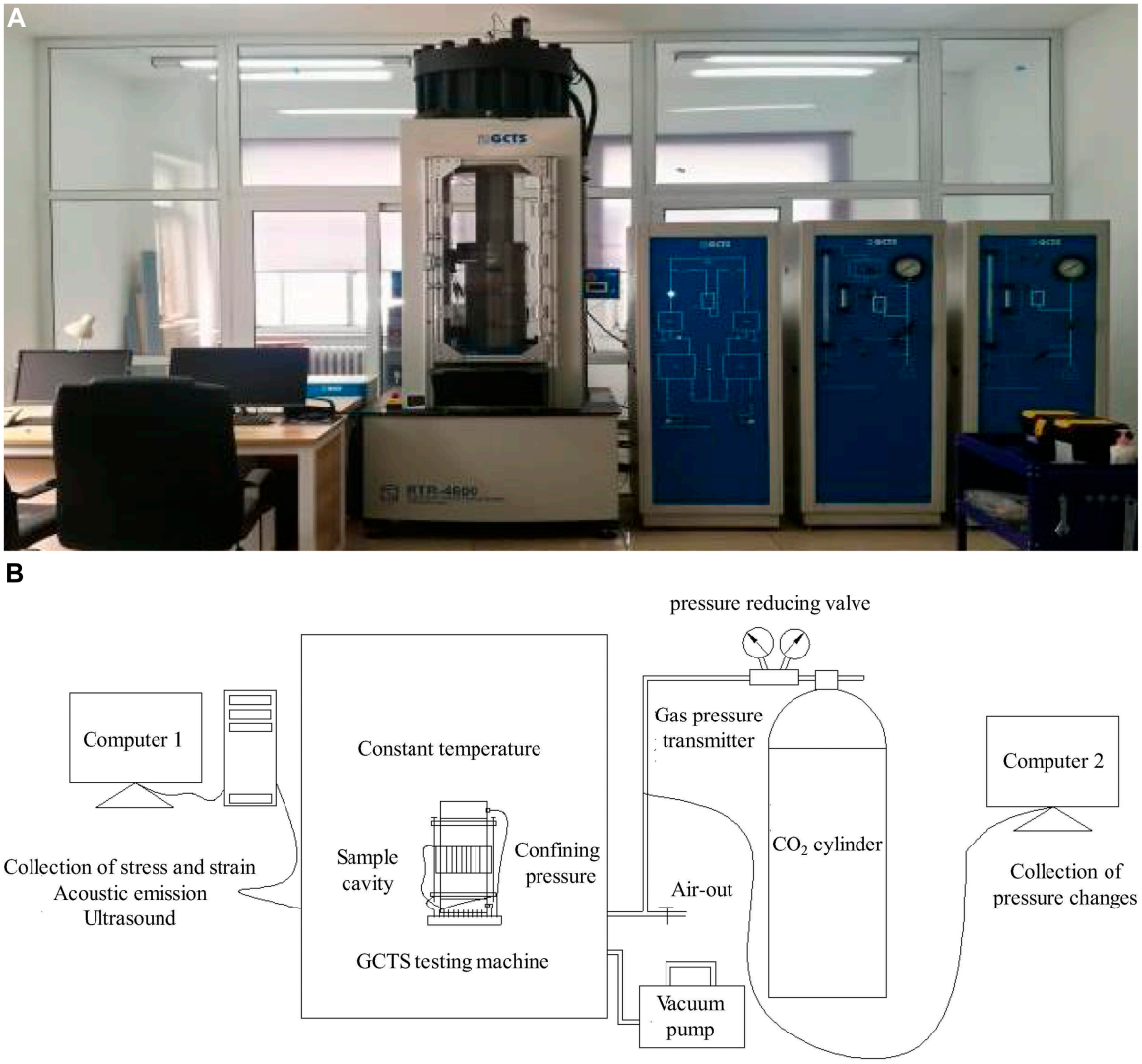

FIGURE 6
Gas-solid coupling test system: **(A)** experimental equipment; **(B)** schematic diagram of the test system.

TABLE 3 Mechanical parameters of coal under different gas pressure.

Sample number	Gas pressure (MPa)	Uniaxial compressive strength (MPa)	Elastic modulus (GPa)	Poisson's ratio
A1~A6	0.0	10.735	2.370	0.343
B1~B5	0.5	10.187	2.288	0.297
C1~C5	1.0	9.033	2.041	0.324
D1~D5	2.0	7.836	1.864	0.336

surrounding rock (MPa); λ refers to the coefficient of lateral pressure; r and θ denote the polar coordinates of the micro elements at a certain point in the surrounding rock of the borehole (m, rad).

According to elastic mechanics (Chen, 2007), combined with equilibrium differential equations, geometric equations, physical equations, deformation compatibility equations, and

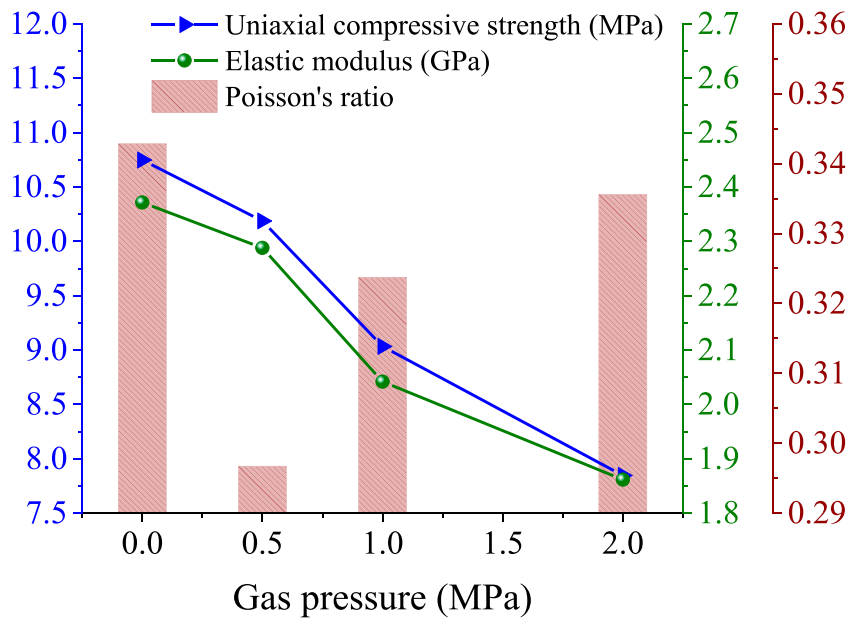

FIGURE 7
The variation of mechanical parameters of coal samples with gas pressure.

boundary conditions, an analytical solution for elastic stress at any point in the borehole surrounding rock can be obtained (Li et al., 2021):

$$\begin{cases} \sigma_r = \frac{P}{2}\left[(1+\lambda)\left(1-\frac{a^2}{r^2}\right)-(1-\lambda)\left(1-4\frac{a^2}{r^2}+3\frac{a^4}{r^4}\right)\cos 2\theta\right] \\ \sigma_\theta = \frac{P}{2}\left[(1+\lambda)\left(1+\frac{a^2}{r^2}\right)+(1-\lambda)\left(1+3\frac{a^4}{r^4}\right)\cos 2\theta\right] \\ \tau_{r\theta} = \frac{P}{2}\left[(\lambda-1)\left(1+2\frac{a^2}{r^2}-3\frac{a^4}{r^4}\right)\sin 2\theta\right] \end{cases} \quad (1)$$

where σ_r and σ_θ represent radial stress and shear stress, respectively (MPa); a denote the radius of borehole (m).

4.2 Limit equilibrium zone of borehole surrounding rock

Assuming that the gravity of the rock within the model range can be ignored, the equilibrium differential equation can be obtained based on the stress analysis of the micro elements of the borehole surrounding rock:

$$(\sigma_r + \mathrm{d}\sigma_r)(r+\mathrm{d}r)\mathrm{d}\theta - \sigma_r r\mathrm{d}\theta - 2\sigma_\theta \mathrm{d}r \sin\frac{\theta}{2} = 0 \quad (2)$$

Ignoring the high-order differential term in Eq. 2, the equilibrium differential equation can be simplified as:

$$\frac{\partial \sigma_r}{\partial r} + \frac{\sigma_r - \sigma_\theta}{r} = 0 \quad (3)$$

According to the Mohr-Coulomb criterion of rock failure, the equilibrium differential equation of the plastic zone microelement is obtained:

$$(\sigma_r + C\cot\eta)(1+\sin\eta) - (\sigma_\theta + C\cot\eta)(1-\sin\eta) = 0 \quad (4)$$

where C refers to the cohesive force of the surrounding rock (MPa); η denotes the internal friction angle of the surrounding rock (°).

Combining Eqs 3, 4, it can be obtained:

$$\frac{\mathrm{d}\sigma_r}{\sigma_r + C\cot\eta} = \frac{2\sin\eta}{1-\sin\eta}\frac{\mathrm{d}r}{r} \quad (5)$$

Perform integral solution on Eq. 5:

$$\sigma_r + C\cot\eta = Ar^{\frac{2\sin\eta}{1-\sin\eta}} \quad (6)$$

where A is the parameter generated by the integration process. When r = a, σ_r = 0, substituting this boundary condition into Eq. 6 yields:

$$A = \frac{C\cot\eta}{a^{\frac{2\sin\eta}{1-\sin\eta}}} \quad (7)$$

Substituting Eq. 7 into Eq. 6, the radial stress expression of coal at the boundary in the plastic zone is obtained:

$$\sigma_r = C\cot\eta\left(\frac{r}{a}\right)^{\frac{2\sin\eta}{1-\sin\eta}} - C\cot\eta \quad (8)$$

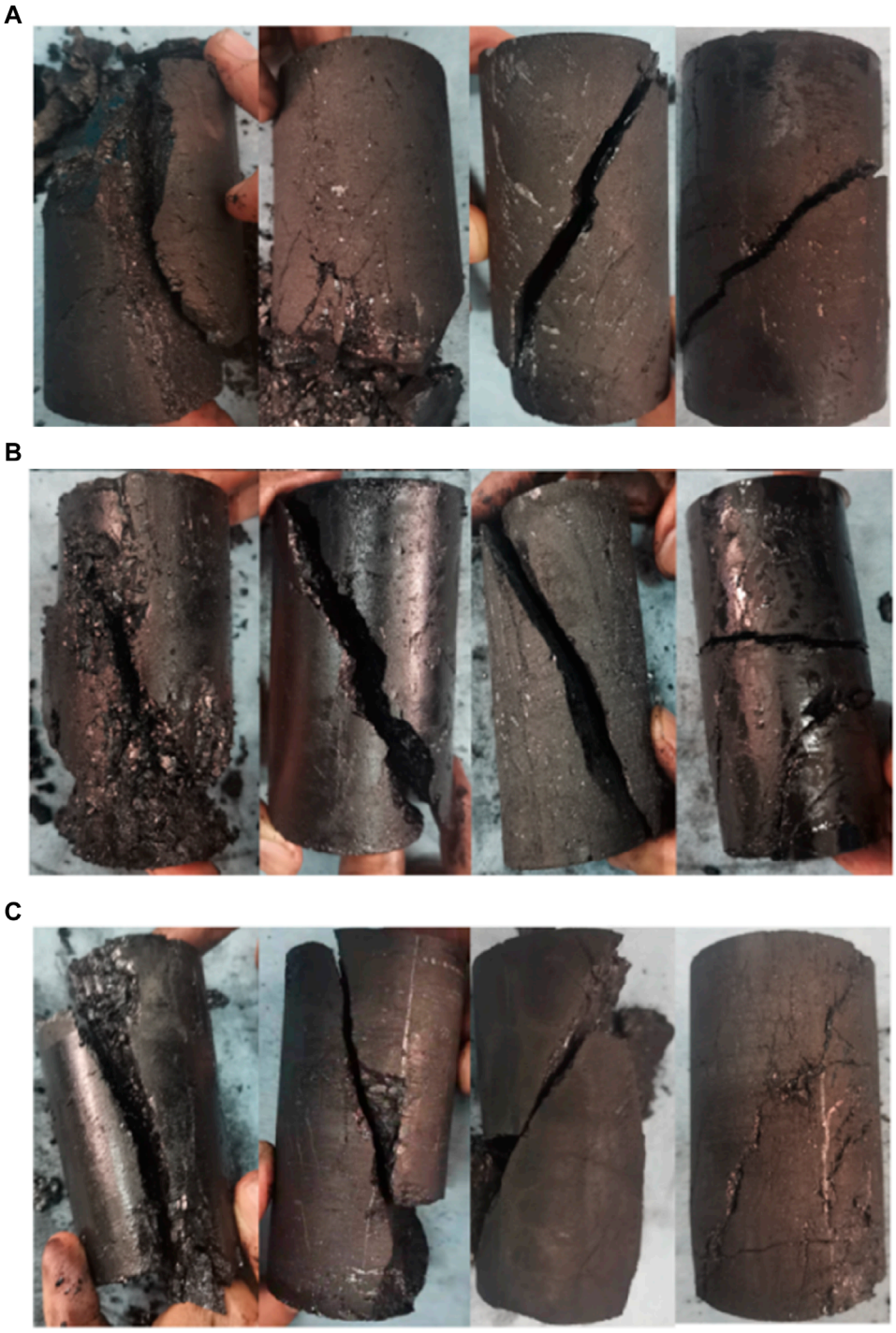

FIGURE 8
Failure pictures of samples under different confining pressures and gas pressures: **(A)** 3.5 MPa confining pressure; **(B)** 4.4 MPa confining pressure; **(C)** 5.3 MPa confining pressure.

Substituting Eq. 8 into Eq. 4, the circumferential stress of coal at the boundary of the plastic zone can be expressed as:

$$\sigma_\theta = \frac{1+\sin\eta}{1-\sin\eta} C\cot\eta\left(\frac{r}{a}\right)^{\frac{2\sin\eta}{1-\sin\eta}} - C\cot\eta \tag{9}$$

Then, the boundary equation of the plastic zone can be obtained by substituting Eq. 1 into Eq. 4:

$$\left\{\frac{P}{2}\left[(1+\lambda)\left(1-\frac{a^2}{R^2}\right)-(1-\lambda)\left(1-4\frac{a^2}{R^2}+3\frac{a^4}{R^4}\right)\cos 2\theta\right]+C\cot\eta\right\}(1+\sin\eta)$$
$$-\left\{\frac{P}{2}\left[(1+\lambda)\left(1+\frac{a^2}{R^2}\right)+(1-\lambda)\left(1+3\frac{a^4}{R^4}\right)\cos 2\theta\right]+C\cot\eta\right\}(1-\sin\eta)=0 \tag{10}$$

where R denotes the boundary radius of the plastic zone (m). The analytical expression for the boundary radius R of the plastic zone

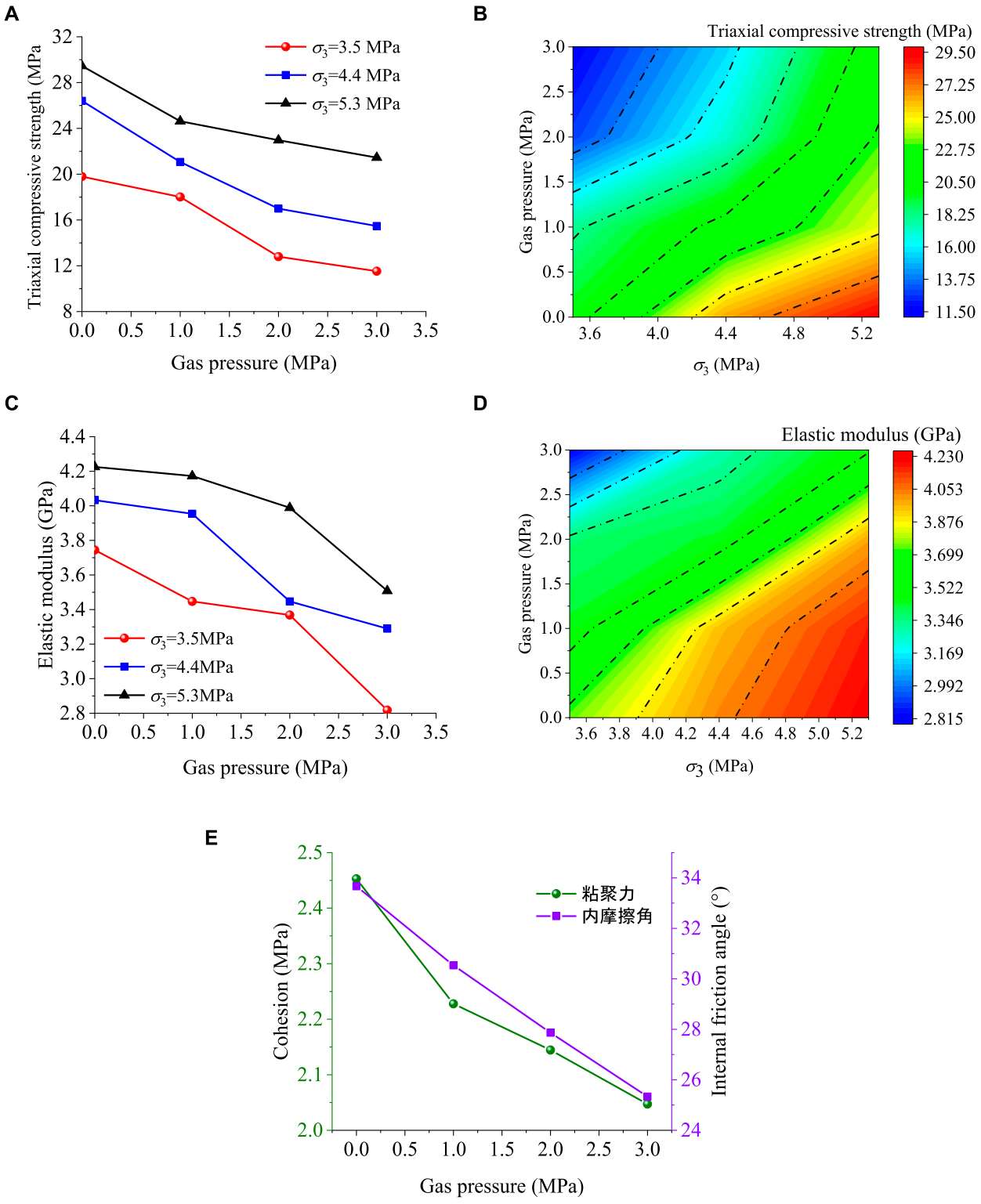

FIGURE 9
Influence of gas pressure on mechanical properties of coal: **(A)** strength and gas pressure curves; **(B)** strength and gas pressure cloud chart; **(C)** elastic modulus and gas pressure curves; **(D)** elastic modulus and gas pressure cloud chart; **(E)** curves of cohesion, internal friction angle, and gas pressure.

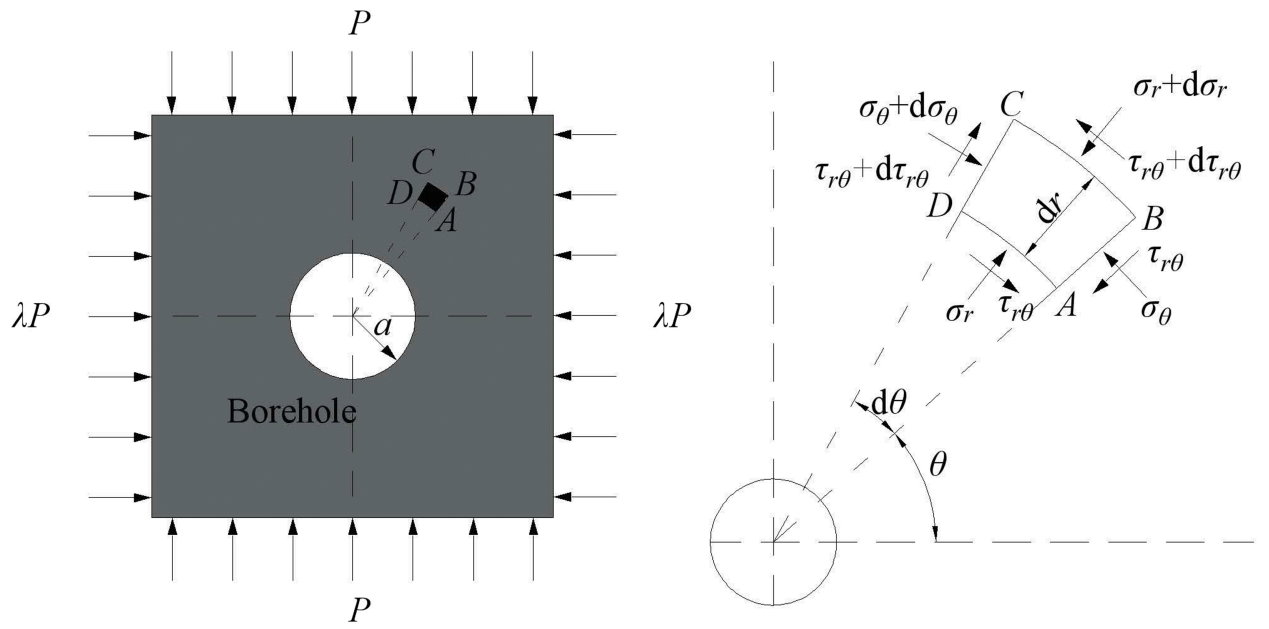

FIGURE 10
Mechanical model of borehole surrounding rock.

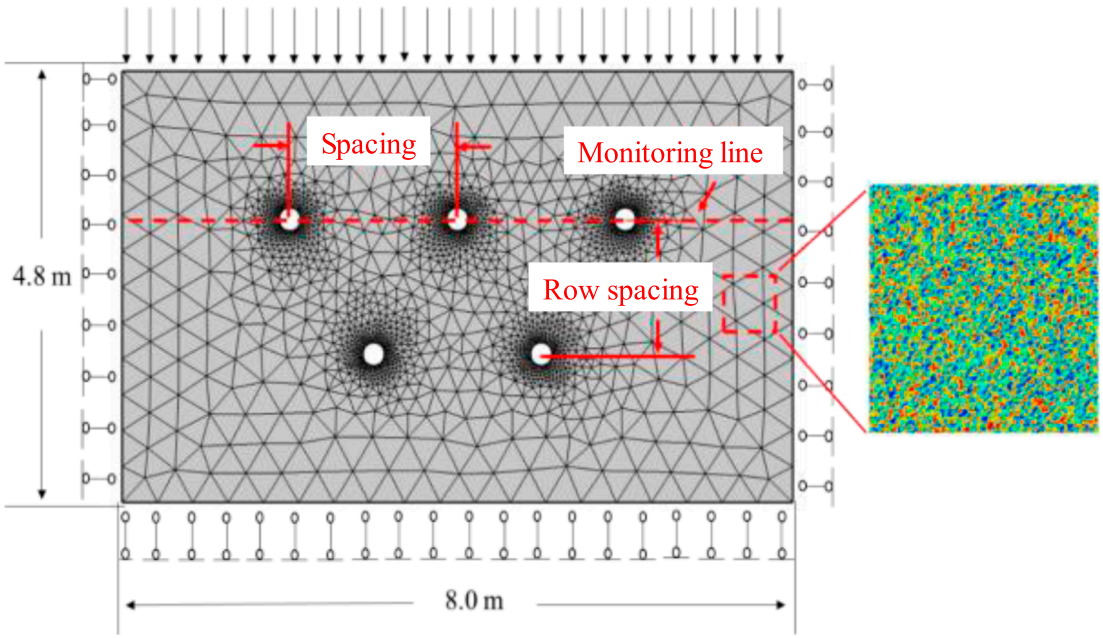

FIGURE 11
Numerical geometric model.

TABLE 4 Numerical simulation parameters.

Parameter	Numerical value	Unit
Initial porosity	0.05	—
Initial permeability	1×10^{-18}	m^2
Elastic modulus	1.47	GPa
Cohesion	3.1	MPa
Internal friction angle	27.1	°
Poisson's ratio	0.34	—
Coal density	1,400	$kg\cdot m^{-3}$
Gas density under standard atmospheric pressure	0.657	$kg\cdot m^{-3}$
Gas dynamic viscosity coefficient	1.22×10^{-5}	Pa·s
Langmuir pressure constant	4.3	MPa
Langmuir volumetric strain constant	0.01266	—
Biot coefficient	1	—
Initial gas pressure	1	MPa
Compressive coefficient of coal cleat cracks	0.045	MPa^{-1}

can be obtained by solving Eq. 10.

$$R = \pm\sqrt{6}a\sqrt{\frac{\pm P(\lambda-1)(2\cos^2\theta-1)}{3P-P\lambda+\sqrt{w}+2P\sin\eta-4P\cos^2\theta+4P\lambda\cos^2\theta-4P\cos^2\theta\sin\eta-2P\lambda\sin\eta+4P\lambda\cos^2\theta\sin\eta}}$$

$$\begin{aligned} w = {} & 8P^2\cos^2\theta-16P^2\cos^4\theta-4P^2\cos^2\eta+10P^2\lambda+P^2- \\ & 7P^2\lambda^2-16P^2\cos^2\eta\sin\eta-4P^2\lambda^2\cos^2\eta \\ & +16P^2\cos^2\theta\cos^2\eta-16P^2\cos^4\theta\cos^2\eta-16P^2\lambda\sin\eta \\ & -32P^2\lambda\cos^2\theta+32P^2\lambda\cos^4\theta+8P^2\lambda\cos^2\eta \\ & +16P^2\lambda^2\sin\eta-24CP\cos\eta+24P^2\lambda^2\cos^2\theta-16P^2\lambda^2\cos^4\theta \\ & +16P^2\lambda^2\cos^2\theta\cos^2\eta-16P^2\lambda^2\cos^4\theta\cos^2\eta \\ & +24CP\lambda\cos\eta+64P^2\lambda\cos^2\theta\sin\eta-64P^2\lambda\cos^4\theta\sin\eta \\ & -32P^2\lambda\cos^2\theta\cos^2\eta+2P^2\lambda\cos^4\theta\cos^2\eta \\ & -48P^2\lambda^2\cos^2\theta\sin\eta+32P^2\lambda^2\cos^4\theta\sin\eta \\ & +48CP\cos^2\theta\cos\eta-48CP\lambda\cos^2\theta\cos\eta \end{aligned} \tag{11}$$

From the expression of plastic zone boundary radius R in Eq. 11, it can be seen that the plastic zone boundary radius of borehole surrounding rock is mainly affected by the vertical pressure P, lateral pressure coefficient λ, borehole radius a, cohesion of borehole surrounding rock C, and internal friction angle η. Among them, the vertical pressure P and lateral pressure coefficient λ of the borehole surrounding rock are determined by the stress environment of the coal, and the cohesion C and internal friction angle η of the borehole surrounding rock are the mechanical properties of the borehole surrounding rock itself. For non-group coal seam mining, high gas and outburst mines, its crustal stress environment is difficult to change. The aperture of the drainage and pressure relief boreholes is fixed. The radius of the pressure relief zone is related to parameters such as cohesion C and internal friction angle η. The research in Section 2.3 of this paper indicates that the greater the gas pressure, the smaller the cohesion C and internal friction angle η of coal.

5 Impact of drainage boreholes on coal stress environment

To verify the coupling mechanism of anti-rockburst and pressure relief effect of boreholes along seam on coal, a two-dimensional plane model (8 m×4.8 m) was established using the gas-solid coupling module of COMSOL software. A vertical stress of 15 MPa is applied to the upper boundary of the model, while other boundaries are supported by rollers, as shown in Figure 11. The model assumes an initial porosity of 0.05 and an initial permeability of 1×10^{-18} m^2. The aperture, spacing, and row spacing of the drainage boreholes in the model are set to 130, 1.5, and 1.5 m, and the gas pressure is set to 1.0 MPa, 2.0 MPa, and 3.0 MPa, respectively. The pressure at the boundary of the borehole is 1.5×10^4 Pa to simulate negative pressure gas drainage. There is a gas pressure difference between inside the coal seam and outside the borehole, leading to gas release and desorption. Considering the non-uniformity of the elastic modulus and cohesion of coal, the physical and mechanical parameters of coal and gas in the model are detailed in Table 4. The influence of gas pressure on the

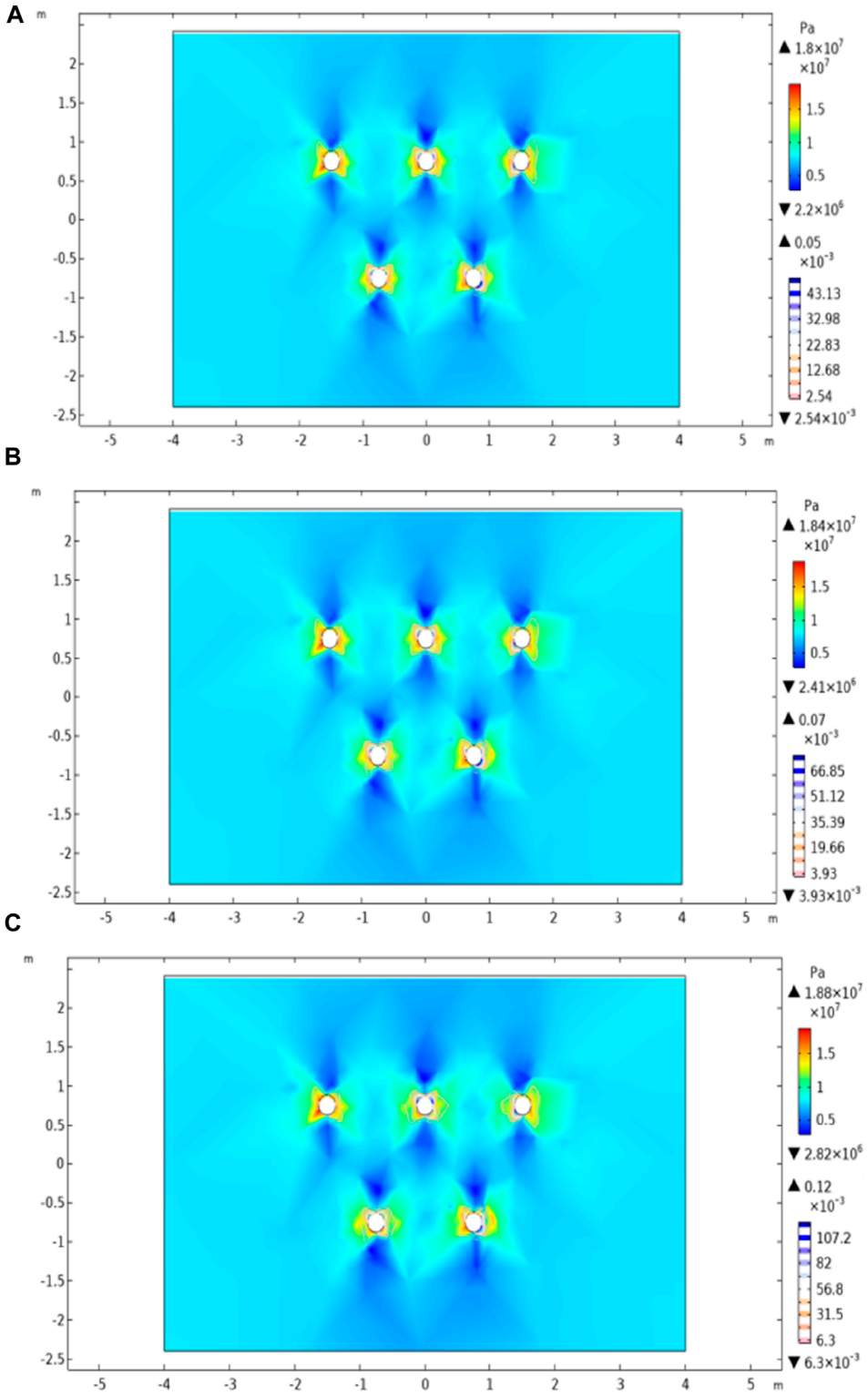

FIGURE 12
Stress-plastic strain cloud diagram of coal under different gas pressure: **(A)** 1.0 MPa gas pressure; **(B)** 2.0 MPa gas pressure; **(C)** 3.0 MPa gas pressure.

stress field and plastic strain of coal is analyzed through numerical simulation.

The distribution of stress and plastic strain in coal under different coal seam gas pressures is shown in Figure 12. The stress in the coal around the boreholes is significantly higher than that in other positions. Besides, with the increase of gas pressure in the coal seam, the peak stress and the peak value of plastic strain of coal in the cloud diagram gradually increase. The stress

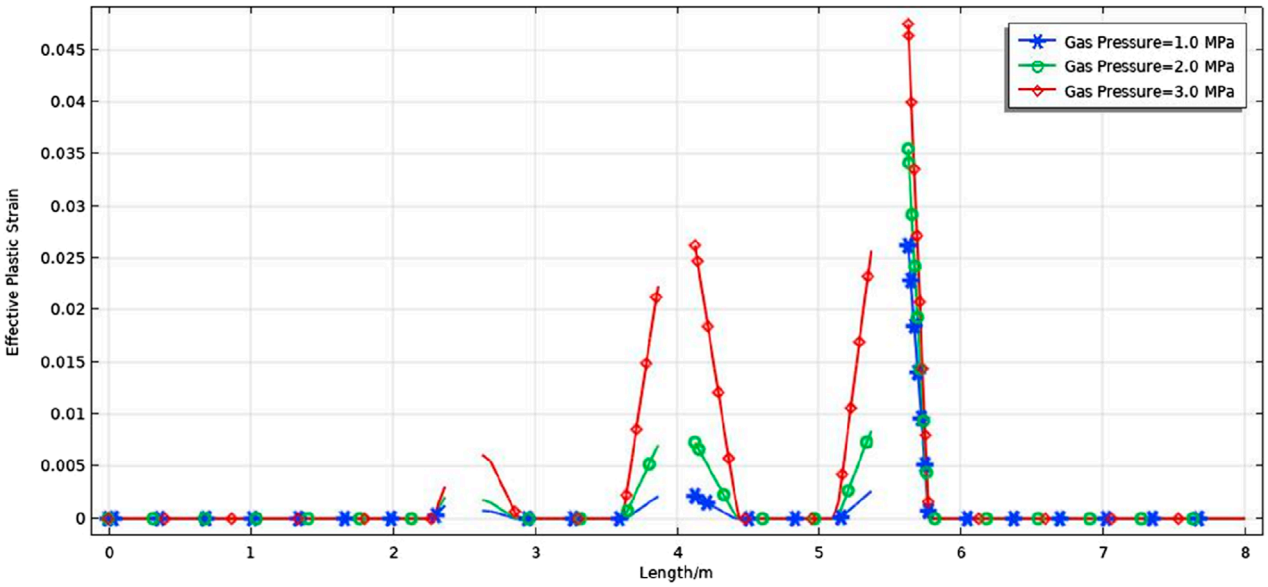

FIGURE 13
Plastic strain line diagram of coal.

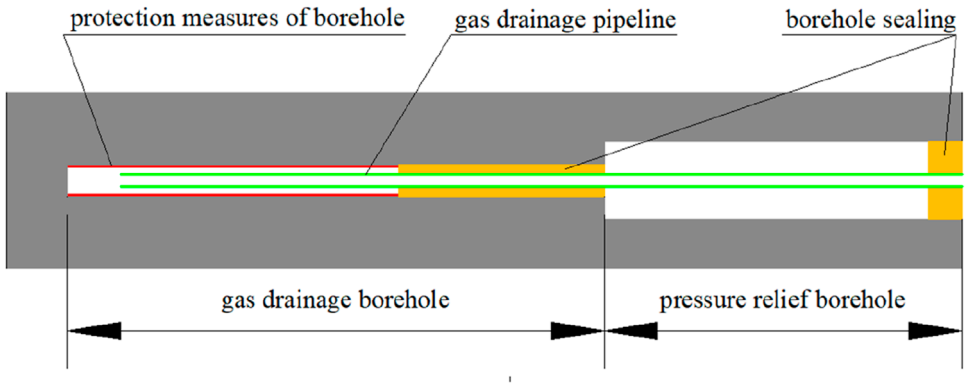

FIGURE 14
Schematic diagram of borehole layout.

in areas not affected or less affected by boreholes in the coal seam gradually increases with the increase of gas pressure, that is, the increase of gas pressure causes the overall stress in the coal seam to rise.

In order to analyze the impact of gas pressure on the stress and plastic strain around the borehole, the stress and plastic strain data of coal under different gas pressures at the monitoring line in Figure 11 were picked up. As shown in Figure 13, there is significant plastic strain generated around the boreholes, and the plastic strain far from the boreholes is small or do not reach the yield state. From the numerical simulation results of strain and plastic strain in the figure, it can be found that the mechanical response of the coal seam is different as the gas pressure in the coal seam increases, that is, the greater the gas pressure, the greater the plastic strain around the boreholes.

In summary, the existence of gas pressure within coal not only enhances the overall stress condition of the coal but also diminishes its failure strength. Concurrently, it augments the plastic strain surrounding the drainage boreholes, effectively expanding the radius of pressure relief. This indirectly validates the correctness of the coupling mechanism involved in employing gas drainage boreholes for both anti-rockburst and pressure relief. Furthermore, it underscores the feasibility of utilizing drainage boreholes in gas outburst and rockburst prevention.

6 Discussion

In underground engineering site, schematic diagram of gas drainage and pressure relief borehole layout can be seen in Figure 14. The large diameter pressure relief boreholes along seam were

installed, with a drilling diameter of 150 mm, a drilling sealing length of 2 m at the orifice of pressure relief borehole. Then, the deep extraction boreholes were carried out at the inner end of the pressure relief boreholes, with a drilling diameter of 90 mm, a drilling sealing length of 10 m at the beginning of gas drainage borehole. The gas drainage borehole was carried out protection measures from the end of gas drainage borehole sealing measures to the bottom of gas drainage borehole. The pressure relief borehole can transfer the peak stress of the roadway surrounding rock to depth. The borehole surrounding rock can be compressed or damaged to relieve pressure. The gas drainage borehole was carried out protection measures to ensure the gas extraction. The borehole surrounding rock can be compressed to relieve pressure. The pressure relief effect of gas drainage borehole was weaker than pressure relief borehole, but the stress value was reduced a lot, which can transfer stress peaks to deeper. The borehole causes significant disturbance to the surrounding coal seams, resulting in a wide distribution of fractures and the formation of numerous fractures around the boreholes. The gas seepage channels are formed, causing free gas in deep coal to migrate towards borehole. The gas in drainage borehole was extracted by gas drainage pipeline. The gas in pressure relief borehole act on the coal in the pressure relief zone, which reduced the strength of coal, expands the radius extension range of the pressure relief zone of the borehole, and enhances the effect of pressure relief. Then the peak stress was transferred to the interior of the coal, reducing the range of stress concentration.

7 Conclusion

The issue of rock burst in gas mines is a new scientific challenge that deep mining must face. Its management difficulty is much greater than the prevention and control of a single disaster. This study proposed a multi-drilling combined gas drainage borehole and pressure relief borehole to prevention of rockburst and gas outburst. Then the coupling mechanism of anti-rockburst and pressure relief in gas drainage borehole along seam was studied. The correctness of the coupling mechanism of using multi-drilling for anti-rockburst and pressure relief is indirectly verified. In the future, it is necessary to extend the theory to the field, and truly achieve the dual use of one hole for drainage boreholes through the optimization of onsite process parameters, achieving synchronous management of gas and rockburst disasters.

1. From the perspective of pressure relief, drainage boreholes can reduce the stress environment of coal and further transfer the peak stress of coal to deep coal. Compared to large diameter pressure relief boreholes, drainage boreholes can to some extent reduce the stress of coal. However, due to the small diameter of the drainage boreholes, the pressure relief effect is slightly weaker than that of large diameter pressure relief boreholes.
2. By conducting stress analysis on the surrounding rock of the boreholes and mathematical derivation, the radial and circumferential stress expressions of the boundary coal in the plastic zone of the boreholes surrounding rock were obtained, and the analytical solution of the plastic zone boundary was obtained. The boundary of the plastic zone is influenced by the vertical pressure P, lateral pressure coefficient λ, drilling radius a, cohesion C and internal friction angle η of the borehole surrounding rock.
3. The gas drainage and pressure relief borehole cause significant disturbance to the surrounding coal seams, resulting in a wide distribution of fractures and the formation of numerous fractures around the boreholes. The gas seepage channels are formed, causing free gas in deep coal to migrate towards borehole. The gas in pressure relief borehole act on the coal in the pressure relief zone, which reduced the strength of coal, expands the radius extension range of the pressure relief zone of the borehole, and enhances the effect of pressure relief.

Data availability statement

The raw data supporting the conclusion of this article will be made available by the authors, without undue reservation.

Author contributions

JJ: Writing–original draft, Writing–review and editing, Conceptualization, Data curation, Methodology, Project administration, Resources. ZD: Writing–original draft, Conceptualization, Funding acquisition, Methodology, Project administration, Resources, Writing–review and editing. GZ: Writing–review and editing, Investigation, Project administration, Visualization. SY: Writing–review and editing, Investigation.

Funding

The author(s) declare that financial support was received for the research, authorship, and/or publication of this article. This work was supported by the National Natural Science Foundation of China (Grant Nos. 52034009 and 51874176) and Science and Technology Development Fund Project of China Coal Research Institute (Grant Nos. 2019CX-I-07, 2020CX-II-24 and 2022CX-I-04).

Conflict of interest

The authors declare that the research was conducted in the absence of any commercial or financial relationships that could be construed as a potential conflict of interest.

Publisher's note

All claims expressed in this article are solely those of the authors and do not necessarily represent those of their affiliated

References

Ali, M., Derakhahani, R., Nilfouroushan, F., Rahnamarad, J., and Azarafza, M. (2023). Spatiotemporal subsidence over Pabdana coal mine Kerman Province, central Iran using time-series of Sentinel-1 remote sensing imagery. *Episodes J. Int. Geosci.* 46 (1), 19–33. doi:10.18814/epiiugs/2022/022009

Cai, C., and Zhou, G. (2002). Gas drainage in seam with large auto variable diameter bore holes. *Coal Sci. Techno* 30 (1), 39–41. doi:10.13199/j.cst.2004.12.41.caichg.013

Chen, M. (2007). *Elastic-plastic mechanics*. Beijing, China: Science Press.

Cheng, Y., Yu, Q., Yuan, L., Li, P., Liu, Y., and Tong, Y. (2004). Experimental research of safe and high-efficient exploitation of coal and pressure relief gas in long distance. *J. China Uni Min. Techno* 33 (2), 8–12. doi:10.3321/j.issn:1000-1964.2004.02.002

Ding, H., Jiang, Z., and Han, Y. (2008). Numerical simulation and application of boreholes along coal seam for methane drainage. *J. Univ. Sci. Technol. B* 30 (11), 1205–1210. doi:10.13374/j.issn1001-053x.2008.11.005

Huang, X., and Jiang, C. (2011). Study on sealing technology of gas drainage borehole with pressure in this coal seam. *Coal Sci. Techno* 39 (10), 45–48. doi:10.13199/j.cst.2011.10.50.huangxy.018

Huang, Z., Wan, X., and Kong, L. (2016). Aperture determination and application effect analysis of bedding long boreholes along coal seam for gas pre-drainage. *J. Henan Polytech. Univ. Nat. Sci.* 35 (02), 162–166. doi:10.16186/j.cnki.2016.02.004

Jia, C., Jiang, Y., Zhang, X., Wang, D., Luan, H., and Wang, C. (2017). Laboratory and numerical experiments on pressure relief mechanism of large diameter boreholes. *Chin. J. Geotech. Eng.* 39 (6), 1115–1122. doi:10.11779/CJGE201706018

Lei, C., and Sun, B. (2010). Practice of large diameter drilling to prevent coal and gas outburst. *Min. Saf. Environ. Prot.* 37 (05), 62–64. doi:10.3969/j.issn.1008-4495.2010.05.021

Li, Y., Guo, X., Ma, N., Li, C., and Huo, T. (2021). Research status and evaluation of theoretical calculation of plastic zone boundary for hole surrounding rock. *Coal Sci. Techno* 49 (5), 141–150. doi:10.13199/j.cnki.cst.2021.05.018

Li, Z., Zhang, Y., and Liang, Y. (2021). Mechanism study on compound disaster of rock burst and gas outburst. *Coal Sci. Techno* 49 (07), 95–103. doi:10.13199/j.cnki.cst.2021.07.013

Liu, H., He, Y., Xu, J., and Han, L. (2007). Numerical simulation and industrial test of boreholes destressing technology in deep coal tunnel. *J. China Coal Soc.* 32 (01), 33–37. doi:10.3321/j.issn:0253-9993.2007.01.007

Liu, H., Shu, Z., Shi, Y., Wang, X., Xiao, X., and Lin, J. (2021). Gas migration patterns with different borehole sizes in underground coal seams: numerical simulations and field observations. *Minerals* 11, 1254. doi:10.3390/min11111254

Ma, B., Deng, Z., Zhao, S., and Li, S. (2020). Analysis on the mechanism and influencing factors of drilling pressure relief to prevent rock burst. *Coal Sci. Techno* 48 (05), 35–44. doi:10.13199/j.cnki.cst.2020.05.004

Pan, Y. (2016). Integrated study on compound dynamic disaster of coal-gas outburst and rockburst. *J. China Coal Soc.* 41 (01), 105–112. doi:10.13225/j.cnki.jccs.2015.9034

Pang, L., Fu, S., and Su, B. (2021). Research and application of anti rock burst mechanism of large diameter boreholes in coal seam and roof pre-splitting holes. *Saf. Coal Mines* 52 (09), 183–189. doi:10.13347/j.cnki.mkaq.2021.09.030

Qi, Q., Li, Y., Zhao, S., Zhang, N., Zheng, W., Li, H., et al. (2019). Seventy years development of coal mine rockburst in China: establishment and consideration of theory and technology system. *Coal Sci. Techno* 47 (9), 1–40. doi:10.13199/j.cnki.cst.2019.09.001

Qi, Q., Pan, Y., Li, H., Jiang, D., Shu, L., Zhao, S., et al. (2020a). Theoretical basis and key technology of prevention and control of coal-rock dynamic disasters in deep coal mining. *J. China Coal Soc.* 45 (05), 1567–1584. doi:10.13225/j.cnki.jccs.DY20.0453

Qi, Q., Zhao, S., Li, H., and Qin, K. (2020b). Several key problems of coal bump prevention and control in China's coal mines. *Saf. Coal Mines* 51 (10), 135–143+151. doi:10.13347/j.cnki.mkaq.2020.10.021

Shi, Q., Cui, H., Lv, D., Pan, J., Xia, Y., and Wang, S. (2017). Study on pressure relief drilling holes layout parameters of roadside in rockburst coal seam. *Coal Min. Techno* 22 (06), 74–77. doi:10.13532/j.cnki.cn11-3677/td.2017.06.018

Shi, Z., Yao, N., and Ye, G. (2009). Construction technology and equipment for gas drainage borehole drilling in underground coal mine. *Coal Sci. Techno* 37 (7), 1–4. doi:10.13199/j.cst.2009.07.6.shizhj.028

Wang, L., Liao, X., Chu, P., Zhang, X., and Liu, Q. (2021). Study on mechanism of permeability improvement for gas drainage by cross-seam cavitation borehole. *Coal Sci. Techno* 49 (05), 75–82. doi:10.13199/j.cnki.cst.2021.05.010

Wang, M., Fang, X., Xu, R., and Zhang, X. (2011). Comprehensive gas extraction technology with large aperture and over long directional drilling. *Coal Eng.* 391 (05), 46–48. doi:10.3969/j.issn.1671-0959.2011.05.019

Wang, Q., and Chen, H. (2018). Development and prospect on intelligent drilling technology and equipment for gas drainage. *Industry Mine Automation* 44 (11), 18–24. doi:10.13272/j.issn.1671-251x.17370

Wang, T., Wang, Z., Liu, H., Guan, Y., and Zhan, S. (2014). Discussion about the mechanism of gas disaster induced by coal bump. *J. China Coal Soc.* 39 (2), 371–376. doi:10.13225/j.cnki.jccs.2013.2021

Wang, X., Zhou, H., Zhang, L., Hou, W., and Cheng, J. (2022). Dual-zone gas flow characteristics for gas drainage considering anomalous diffusion. *Energies* 15, 6757. doi:10.3390/en15186757

Xie, H., Zhou, H., Xue, D., Wang, H., Zhang, R., and Gao, F. (2012). Research and consideration on deep coal mining and critical mining depth. *J. China Coal Soc.* 37 (4), 535–542. doi:10.13225/j.cnki.jccs.2012.04.011

Xu, M., Lin, H., Li, S., and Hu, A. (2010). Study on influencing rule of coal-bed methane pre-drainage by boreholes. *Min. Saf. Environ. Prot.* 37 (5), 1–3. doi:10.3969/j.issn.1008-4495.2010.05.001

Yu, B., and Wang, Y. (2005). *Technical manual for mine gas disaster prevention and utilization*. Beijing, China: China Coal Industry Publishing House.

Yuan, L. (2015). Strategic thinking of simultaneous exploitation of coal and gas in deep mining. *J. China Coal Soc.* 41 (1), 1–6. doi:10.13225/j.cnki.jccs.2015.9027

Yuan, L., Lin, B., and Yang, W. (2015). Research progress and development direction of gas control with mine hydraulic technology in China Coal Mine. *Coal Sci. Techno* 43 (1), 45–49. doi:10.13199/j.cnki.cst.2015.01.011

Zhang, C., Xu, J., Peng, S., Li, Q., and Yan, F. (2019). Experimental study of drainage radius considering borehole interaction based on 3D monitoring of gas pressure in coal. *Fuel* 239, 955–963. doi:10.1016/j.fuel.2018.11.092

Zhang, M. (1987). Instability theory and mathematical model for coal/rock bursts. *Chin. J. Rock Mech. Eng.* 6 (3), 197–204.

Zhao, H., Li, J., Liu, Y., Wang, Y., and Cheng, H. (2020). Experimental and measured research on three-dimensional deformation law of gas drainage borehole in coal seam. *Int. J. Min. Sci. Techno* 30 (3), 397–403. doi:10.1016/j.ijmst.2020.04.001